

at the base of the vascular bundles as reported earlier⁷ and this formed a cambium-like layer which later spread rapidly. Microscopy observations of development of callus in the young shoot buds revealed that meristemoids were formed from xylem parenchyma as indicated.

The present communication shows effectiveness of using sprouted buds on the nodal explants of 8–10-year-old, mature bamboo for induction of somatic embryos and also increasing their conversion frequency into plantlets by incorporating high sucrose concentration in the medium. Once the plantlets are formed, these could further be multiplied in static liquid media wherein, prolonged sub-culturing resulted in rhizome formation. The segments from the latter could also be used for further multiplication of the species.

1. Sood, A., Palni, L. M. S., Sharma, M. and Sharma, O. P., in *Biotechnology in India* (ed. Dwivedi, B. K.), Bioved. Res. Soc., Allahabad, 1994, pp. 199–212.
2. Murashige, T. and Skoog, F., *Physiol. Plant.*, 1962, **15**, 473–497.
3. Mehta, U., Rao, I. V. R. and Mohan Ram, H. Y., in Proceedings of the Fifth International Congress on Plant Tissue Culture (ed. Fujiwara, A.), Tokyo, 1982, pp. 109–110.
4. John, C. K., Nadgauda, R. S. and Mascarenhas, A. F., in *Forest Trees Tissue Culture of Economic Plants*, Centre for Science and Technology of the Non-Aligned and Other Developing Countries and Commonwealth Science Council, London, 1997, pp. 42–81.
5. Mascarenhas, A. F. *et al.*, in Proceedings of the International Bamboo Workshop (eds Ramanuja, I. V. R., Gnanaharan, R. and Sastry, B.), KFRI, Peechi and IDRC, Canada, 1988, pp. 159–166.
6. Chaturvedi, H. C., Sharma, M. and Sharma, A. K., *Plant Sci.*, 1993, **91**, 97–101.
7. Rao, I. V. R. and Rao, U. I., see ref. 5, pp. 151–158.
8. Nadgir, A. L., Phadke, C. H., Gupta, P. K., Parsharami, V. A., Nair, S. and Mascarenhas, A. F., *Silvae Genet.*, 1984, **33**, 219–223.
9. Woods, S. H., Phillips, G. C., Woods, J. E. and Collins, G. B., *Plant Cell Rep.*, 1992, **11**, 257–261.
10. Samora, A. B., Gruezo, S. S. and Damasco, O. P., *Phillip. Agri.*, 1988, **71**, 76–84.
11. Huang, L. C., Huang, B. L. and Chess, W. L., *Environ. Exp. Bot.*, 1989, **29**, 307–315.
12. Rao, I. U. R., Rao, I. V., Narang, V., Jerath, R. and Pillai, K. G., see ref. 5, pp. 167–172.
13. Ramkers, K., Jacobsen and Visser, R., in *Somatic Embryogenesis in Woody Plants* (eds Jain, S. M., Gupta, P. K. and Newton, R. J.), Kluwer Academic Publishers, Dordrecht, 1999, vol. 4, pp. 29–59.
14. Kumar, A., Sood, A., Palni, L. M. S. and Gupta, A. K., *Plant Cell Tissue Org. Cult.*, 1999, **57**, 105–112.
15. Nonohay, J. S., Mariath, J. E. A. and Winge, H., *Plant Cell Rep.*, 1999, **18**, 929–934.
16. Shirgurkar, M. V., Thengane, S. R., Poonawala, I. S., Jana, M. M., Nadgauda, R. S. and Mascarenhas, A. F., *Curr. Sci.*, 1996, **70**, 940–943.
17. Rout, G. R. and Das, P., *Plant Cell Rep.*, 1994, **13**, 683–686.

ACKNOWLEDGEMENTS. We are grateful to Department of Biotechnology (GOI), New Delhi for financial help by way of research grant and to Dr R. D. Singh, HATS Division, Institute of Himalayan Bioresource Technology for help in statistical analysis.

Received 17 April 2002; revised accepted 2 August 2002

Origin of ash in the Central Indian Ocean Basin and its implication for the volume estimate of the 74,000 year BP Youngest Toba eruption

J. N. Pattan^{†,*}, N. J. G. Pearce[#], V. K. Banakar[†] and G. Parthiban[†]

[†]National Institute of Oceanography, Dona Paula, Goa 403 004, India

[#]Institute of Geography and Earth Sciences, University of Wales, Aberystwyth, SY23 3DB, UK

A controversy exists about the origin of ash in the Central Indian Ocean Basin (CIOB). *In situ* silicic volcanism and Indonesian arc volcanism have been proposed as sources of ash in the basin. We present here the detailed morphology and chemical composition (ten major, 20 trace and 14 rare earth elements (REE)) of glass shards from eight sediment cores in the CIOB to gain insights and provide new estimates of ash volume. The glass shards are of rhyolitic composition with a strong negative Europium anomaly, and show a bubble wall junction-type morphology suggesting a magmatic type of eruption. Major, trace and REE composition and morphology of the shards suggest Youngest Toba Tuff (YTT) of ~74 ka of Northern Sumatra as the source for the ash. The YTT shards have higher Ca, K, Al, Cs, Ba, Ta, Th, U and heavy REE and lower Fe, Rb, Sr, Y and light REE compared to Middle Toba Tuff, and higher Si, K, Hf and light REE, and lower Ti, Fe, Mn, Mg, Ca, Na, Rb, Sr, Y, Nb, Th, U and heavy REE compared to Oldest Toba Tuff. The YTT covers a new minimum area of ~3.2 × 10⁶ km² in the CIOB and increases additional ash volume by 160 km³ to the earlier volume (350 km³) reported. The new occurrence of YTT from the CIOB, South China Sea and Arabian Sea suggests significant increase in ash volume, and climatic implications need to be reassessed.

ASH layers in the marine sedimentary records are important because they provide information about cyclicity of volcanism, volcanic production rate and volume, eruption duration, geochemical character of source, and temporal relations between palaeoclimate and volcanic history^{1,2}. Chemical composition, age and morphology of volcanic products far removed from their sources can be used to identify the sources. There is controversy regarding the source of ash in the Central Indian Ocean Basin (CIOB). Different sources such as *in situ* silicic volcanism^{3–5} and Indonesian arc volcanism^{6,7} have been suggested. Martin-Barajas and Lallier-Vergas⁶ suggested Indonesian arc volcanism as the source for the ash but the low alkali content of their analysis did not allow them to correlate with the Youngest Toba Tuff (YTT). Here, we present

*For correspondence. (e-mail: Pattan@csnio.ren.nic.in)

RESEARCH COMMUNICATIONS

detailed work on morphology and chemical composition (ten major, 20 trace and 14 rare earth elements) of glass shards separated from ash layers from eight sediment cores in the CIOB, in an attempt to identify the source and estimate ash volume.

Seven sediment cores in the abyssal siliceous ooze from a water depth of > 4900 m and one core from a water depth of 4300 m (above the carbonate compensation depth) were collected during various cruises in the CIOB (Table 1, Figure 1). Ash layer occurs between 10 and 35 cm depth in the siliceous ooze, except in core NR-01 where it is exposed at the surface due to erosion of younger sediment⁸. In the carbonate sediment core, ash layer occurs at a depth of 112–125 cm due to higher sedimentation rate. The coarse fraction (> 63 µm) from ash layers was obtained by wet-sieving the bulk sedi-

Table 1. Location and other details of sediment cores from the Central Indian Ocean Basin

Core no.	Latitude (S)	Longitude (E)	Water depth (m)	Core length (cm)	Interval of ash occurrence (cm)
CR-02	03°00'	82°15'	4900	470	20–28
CR-05	03°00'	88°00'	4300	130	112–125
NR-01	09°56'	77°42'	5250	41	0–10
NR-21	11°30'	78°32'	5325	35	20–30
NR-35	11°56'	78°29'	5450	28	14–26
NR-54	07°00'	78°15'	5200	70	30–35
SK-226	13°08'	75°00'	5270	36	18–26
SS-657	14°00'	76°00'	5050	36	6–14

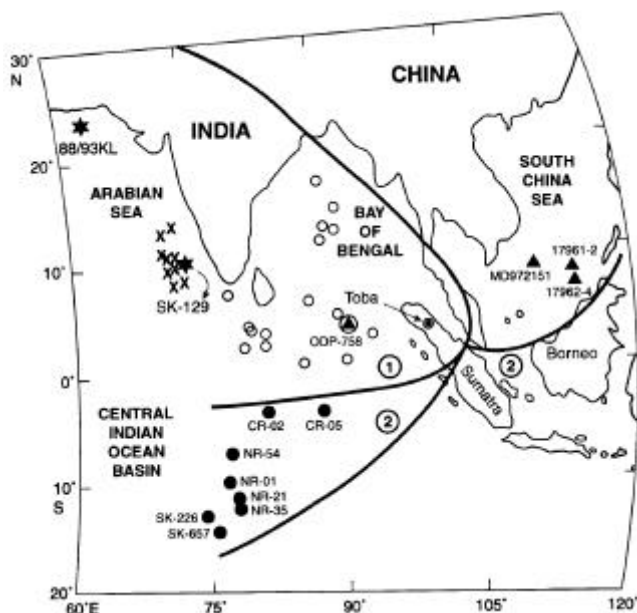


Figure 1. Location map showing the occurrence of Youngest Toba ash in the Central Indian Ocean Basin (present study), Bay of Bengal^{14,20}, South China Sea^{16,18} and Arabian Sea^{17,19,21}. Line 1 is the earlier area demarcated by the occurrence of YTT and line 2 is the extension of new occurrence.

ment. Microscopic observation of coarse fraction revealed the presence of radiolarians, manganese micronodules and glass shards with varying abundance. The glass shards were separated using heavy liquid bromoform and cleaned ultrasonically. Morphology of the glass shards was studied by Scanning Electron Microscopy (Leica-440). Major element composition of glass shards was obtained by electron microprobe⁷. Twenty trace and 14 rare earth elements (REE) were determined using a VG Elemental Plasma Quad II+ Inductively Coupled Plasma-Mass Spectroscopy with a modified high sensitivity

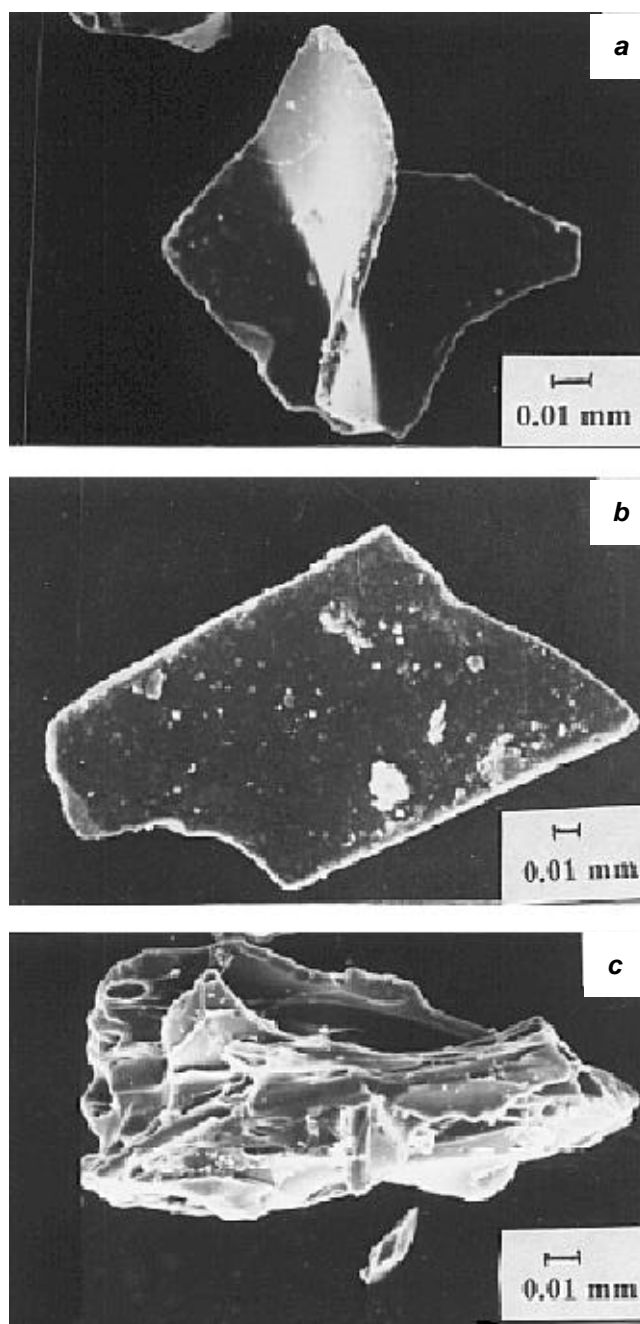


Figure 2. Scanning electron microphotographs of glass shards. *a*, Cusped shape; *b*, Flat shape, and *c*, Pumice with elongated vesicles.

interface, using fully quantitative solution analysis methods described earlier^{9,10}.

Megascopically, the ash layer is light grey in colour, individual glass shards under microscope are colourless,

Table 2. Average major element composition (wt.%) of glass shards from the CIOB compared with the YTT from other locations

Oxide	1	2	3	4	5
SiO ₂	76.81 (0.22)	77.58 (0.23)	77.08 (0.16)	77.48	77.06
Al ₂ O ₃	12.77 (0.12)	12.60 (0.13)	12.60 (0.09)	12.42	12.44
TiO ₂	0.07 (0.04)	0.06 (0.04)	0.05 (0.03)	0.05	0.11
FeO	0.92 (0.07)	0.90 (0.05)	0.90 (0.04)	0.85	0.88
MnO	0.06 (0.04)	0.06 (0.03)	0.07 (0.02)	0.07	0.11
MgO	0.05 (0.03)	0.05 (0.02)	0.05 (0.01)	0.05	0.06
CaO	0.79 (0.07)	0.77 (0.07)	0.78 (0.06)	0.75	0.80
Na ₂ O	3.41 (0.13)	3.24 (0.13)	3.24 (0.10)	2.43	3.36
K ₂ O	5.08 (0.16)	4.96 (0.14)	5.06 (0.13)	4.72	5.11
Cl	0.16 (0.03)	0.14 (0.03)	0.16 (0.03)	–	0.12
H ₂ O	5.23 (0.97)	1.99 (0.86)	4.22 (0.33)	–	4.94
N	91	274	72	53	16

1, Central Indian Ocean Basin⁷ (present study); 2, YTT from Sumatra, Malaysia, Bay of Bengal and India¹⁰; 3, YTT from the Indian subcontinent¹⁵; 4, YTT from South China Sea^{16,18}; YTT from Arabian Sea^{19,21}. Analysis presented as mean and standard deviation (in parenthesis). N, Number of individual shards analysed; –, No data.

fresh, without any oxide coatings, lack cracks/fractures, are isotropic and unaltered. Rose and Chesner¹¹ carried out an extensive study of glass shards for their shape, size, diameter, area and perimeter from the Northern Indian Ocean. Majority of the glass shards are of the bubble wall junction-type, i.e. cusped/lunate or flat (Figure 2). Pumice shards with cellular and elongated parallel vesicles are present (Figure 2). The cusped-type glass shards are formed due to fragmentation of two or three adjacent bubbles during eruption, while the flat shards are formed by the fragmentation of large flattened glass. The ash has been classified into two types: (1) magmatic type, formed due to the loss of coherence in froth magma during its ascent to the ground surface, and (2) phreatomagmatic type, formed due to fragmentation of quenched magma as a result of quick chilling through contact with water. Such fragmentation of quenched magma invariably forms small blocky or pyramidal shape glass shards¹². The bubble wall junction-type morphology and absence of blocky or pyramidal morphology of the glass suggest magmatic origin. The absence of droplet-shaped morphology indicates a high viscosity magma¹².

Table 3. Trace and REE composition (ppm) of glass shards from the CIOB compared with the YTT from other locations

Element	CR-02	CR-05	NR-01	NR-21	NR-35	NR-54	SK-226	SS-657	1	2	3	4
Be	2.99	2.44	2.56	2.62	2.65	2.43	2.14	2.42	2.53	–	–	3.02
Sc	1.93	1.55	1.68	1.69	1.89	1.84	1.54	1.93	1.75	–	–	–
V	16.1	14.6	15.4	15.1	17.1	17.4	12.7	15.0	15.5	–	–	–
Cr	2.55	3.21	17.80	4.15	3.86	4.42	12.27	15.12	7.90	–	–	–
Co	0.86	0.61	0.79	0.70	1.23	1.12	0.97	1.16	1.10	–	–	–
Ni	0.76	0.81	3.74	1.25	1.52	1.36	2.99	3.94	2.05	–	–	–
Zn	–	7.33	7.85	9.17	10.17	8.34	6.95	8.81	8.37	–	0.74	–
Cu	3.15	2.43	3.73	3.15	4.76	4.40	5.81	6.20	4.20	–	–	–
Ga	12.3	10.3	10.0	10.4	10.9	10.3	8.3	10.5	10.4	–	–	–
Rb	252	206	213	221	217	206	171	205	211	222	190	245
Sr	63.8	54.9	50.7	53.2	57.1	53.6	43.7	52.2	53.6	42.5	44	66.2
Y	31.7	26.4	27.6	27.7	27.5	26.1	22.0	26.6	26.9	30.7	35	45.2
Zr	87.6	81.6	73.0	75.5	74.6	71.4	57.9	69.9	73.9	76.2	–	97.9
Nb	15.8	12.8	11.5	13.7	13.8	12.5	11.0	12.9	13.0	13.0	16.4	16.1
Cs	10.9	9.0	9.2	9.6	9.4	8.8	7.1	8.8	9.1	7.6	7.4	9.3
Ba	514	427	411	428	444	414	350	414	425	348	364	476
La	33.2	27.0	27.6	28.1	28.6	26.4	21.3	25.9	27.2	29.9	27.4	32.1
Ce	61.8	49.6	50.4	51.8	52.1	48.8	39.4	48.2	50.2	48.8	55.5	52.6
Pr	6.61	5.42	5.32	5.52	5.60	5.36	4.41	5.29	5.40	5.44	6.15	6.60
Nd	22.7	18.6	18.7	19.2	19.3	18.3	15.4	17.3	18.6	19.0	22.0	20.9
Sm	4.71	3.92	3.78	4.02	3.87	3.58	3.37	4.15	3.92	4.06	4.46	4.70
Eu	0.58	0.52	0.45	0.48	0.54	0.46	0.43	0.54	0.50	0.40	0.41	0.65
Gd	4.9	4.0	4.2	4.2	4.2	4.1	3.5	3.9	4.1	4.3	4.6	5.1
Tb	0.87	0.67	0.68	0.69	0.72	0.69	0.56	0.74	0.70	0.73	0.73	0.85
Dy	5.24	4.32	4.46	4.70	4.55	4.39	3.58	4.54	4.47	4.81	4.65	5.71
Ho	1.13	0.92	0.94	1.01	0.98	0.88	0.82	0.94	0.95	1.04	1.00	1.16
Er	3.57	2.95	3.03	3.17	3.15	2.79	2.58	2.97	3.03	3.18	3.01	3.47
Tm	0.75	0.65	0.63	0.64	0.66	0.58	0.52	0.62	0.63	0.53	0.52	0.77
Yb	4.05	3.61	3.42	3.54	3.64	3.18	2.82	3.56	3.85	3.70	3.70	4.01
Lu	0.76	0.61	0.65	0.66	0.69	0.59	0.56	0.61	0.64	0.60	0.57	0.86
Hf	3.71	3.14	3.09	3.27	3.18	2.95	2.80	3.07	3.15	3.15	2.83	3.49
Ta	1.74	1.34	1.18	1.55	1.44	1.29	1.45	1.62	1.45	1.30	1.82	1.46
Th	32.9	25.2	28.4	29.1	29.1	27.7	23.2	28.2	26.7	28.1	30.9	33.1
U	8.1	6.6	7.0	7.4	7.5	6.6	5.9	6.9	6.9	5.1	5.8	6.5

1, Central Indian Ocean Basin (present study, $n = 8$); 2, YTT from Sumatra, Malaysia, ODP site 758, Bay of Bengal and India¹⁰ ($n = 15$); 3, YTT from South China Sea¹⁶ ($n = 2$); 4, YTT from Arabian Sea¹⁹ ($n = 3$); –, Not analysed.

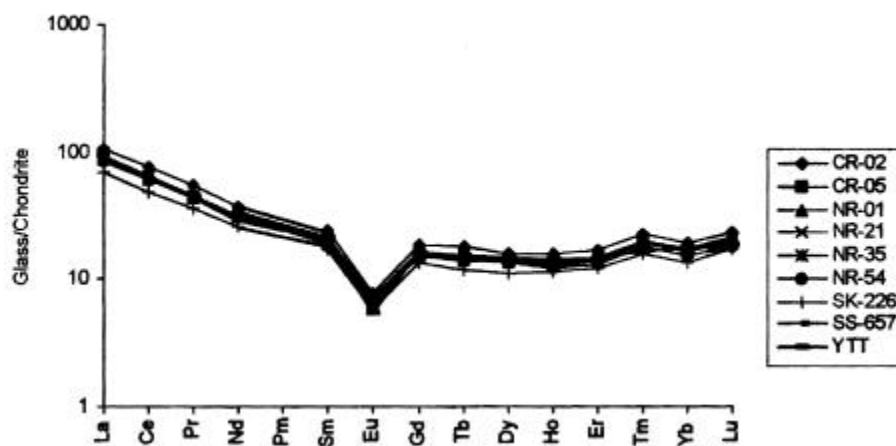


Figure 3. Chondrite-normalized REE patterns of glass shards from the CIOB and YTT published earlier¹⁰.

Analysis of glass shards from tephra deposits by electron microprobe for their major element composition is widely accepted and has been used to identify and distinguish the source of ash beds in sedimentary formations¹³. The CIOB glass shards are high in silica (76.8%) and alkali (8.5%), indicating a rhyolitic composition. They have very low contents of CaO (0.7%), TiO₂ (0.07%), MgO (0.06%), and MnO (0.07%) (Table 2). The major element composition of these glass shards is similar to those reported from Bay of Bengal, Arabian Sea, South China Sea and the Indian subcontinent^{10,11,14–21}. The mean Σ REE concentration of the glass shards from eight sediment cores is 124 ppm (Table 3). It is similar to the Σ REE of the YTT (127 ppm) reported by Westgate *et al.*¹⁰. The chondrite-normalized REE patterns exhibit a strong negative Eu anomaly and show a gradual decrease from La through Sm and nearly constant enrichment from Gd through Lu (Figure 3). The chondrite-normalized ratio of La/Yb (light REE/heavy REE) varies between 4.9 and 5.7 with an average of 5.4, and suggests significant enrichment of light REE over heavy REE. The detailed trace element concentration (Table 3), plot of few selected trace element ratios (La/Lu, Zr/Hf, Nb/Ta, Zr/Nb, Cs/Yb, Ce/Y and Rb/Sr; Figure 4), major elements, REE composition, chondrite-normalized REE pattern and bubble wall junction-type morphology of glass shards from the CIOB match well with proximal sample from Northern Sumatra (Toba caldera) as well as the YTT reported from Bay of Bengal, India, Malaysia, ODP site 758, Arabian Sea and South China Sea^{10,11,14–21}. The Toba caldera of Northern Sumatra eruptions dated ~ 74,000 years BP, ~ 540,000 years BP and ~ 840,000 years BP, are known as the Youngest Toba Tuff (YTT), Middle Toba Tuff (MTT) and Oldest Toba Tuff (OTT) respectively²². The YTT can be distinguished from the MTT and OTT by the chemical composition. The YTT has higher Ca, K, Al, Cs, Ba, Ta, Th, U and heavy REE and lower Fe, Rb, Sr, Y and light REE compared to

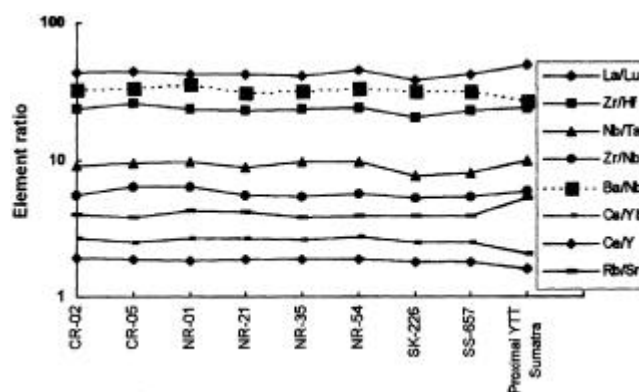


Figure 4. Some trace element ratios of glass shards from the CIOB compared with the YTT from Toba caldera.

MTT, and high Si, K, Hf and light REE, and lower Ti, Fe, Mn, Mg, Ca, Na, Rb, Sr, Y, Nb, Th, U and heavy REE compared to OTT¹⁰.

The YTT eruption from the Toba caldera in Northern Sumatra is the earth's largest volcanic event in the late Quaternary, covering nearly 1% of the earth's surface and its environmental consequences are not fully investigated. The YTT eruption had a duration of 9–14 days²³, with an eruption height of 32–40 km in the stratosphere²⁴. The YTT age was estimated as ~ 74 ka based on K-Ar, ⁴⁰Ar/³⁹Ar, oxygen isotope and biostratigraphy^{10,11,20}. The occurrence of the YTT up to 14°S in the CIOB⁷ suggests ash is dispersed to a distance of ~ 3200 km from the caldera. A distinct aerosol peak of volcanic sulphate at ~ 71,000 years BP in the Greenland GISP2 ice core²⁵, presence of entrapped dust in the Antarctic Vostok ice core at ~ 71,000 years BP²⁶, and a drop in temperature of ~ 4°C at ~ 77,000 years BP²⁷ may be related to the YTT eruption. On the basis of the occurrence of the YTT in the Northern Indian Ocean, Rose and Chesner¹¹ reported a minimum areal coverage of 7×10^6 km² and ash thickness of 10 cm, yielding a minimum ash volume of

350 km³. The minimum area covered by the newly described Youngest Toba ash in the CIOB is estimated to be $\sim 3.2 \times 10^6$ km². In the northern sediment cores the ash thickness is comparatively more (up to 13 cm) and decreases (8 cm) in the southernmost cores, with an average of 10 cm. Based on the area covered in the Southern Hemisphere ($\sim 3.2 \times 10^6$ km²) and average ash thickness (10 cm), the new minimum volume estimate is ~ 160 km³. This volume is in addition to the earlier volume of 350 km³ estimated by Rose and Chesner¹¹ based on the occurrence of ash from the Northern Indian Ocean. Recently, the YTT has been further traced from South China Sea¹⁶ and Arabian Sea^{17,19,21}. For the ash volume estimate, we have not considered locations from South China Sea and Arabian Sea, as data are limited to few stations. Therefore, the new occurrence of the YTT in the CIOB, South China Sea and Arabian Sea suggests significant increase in ash volume estimates, and consequent climatic implications need to be reassessed.

1. Kennett, J. P., in *The Oceanic Lithosphere* (ed. Emiliani, C.), The Sea 7, 1981, pp. 1373–1436.
2. Fischer, R. V. and Schmincke, H. U., *Pyroclastic Rocks*, Springer Verlag, New York, 1984, p. 472.
3. Gupta, S. M., *J. Palaeontol. Soc. India*, 1988, **33**, 59–71.
4. Iyer, S. D., Shyam Prasad, M., Gupta, S. M. and Charan, S. N., *Deep-Sea Res.*, 1997, **44**, 1167–1184.
5. Sukumaran, N. P., Banerjee, R., Borole, D. V. and Gupta, S. M., *Geo-Mar. Lett.*, 1999, **18**, 203–208.
6. Martin-Barajas, A. and Lallier-Vergas, E., *Mar. Geol.*, 1993, **115**, 307–329.
7. Pattan, J. N., Shane, P. and Banakar, V. K., *ibid*, 1999, **155**, 243–248.
8. Banakar, V. K., Gupta, S. M. and Padmavati, V. K., *ibid*, 1991, **96**, 167–173.
9. Pearce, N. J. G., Perkins, W. T., Westgate, J. A., Gorton, M. P., Jackson, S. E., Neal, C. R. and Chenery, S. P., *Geostand. Newsl.*, 1997, **21**, 115–144.
10. Westgate, J. A. *et al.*, *Quat. Res.*, 1998, **50**, 107–122.
11. Rose, W. I. and Chesner, C. A., *Geology*, 1987, **15**, 913–917.
12. Heiken, G., *Geol. Soc. Am. Bull.*, 1972, **83**, 1961–1988.
13. Westgate, J. A. and Gorton, M. P., in *Tephra Studies* (eds Self, S. and Sparks, R. S. J.), Reidel, Dordrecht, 1981, pp. 73–94.
14. Dehn, J., Farrel, J. W. and Schmincke, H. U., Proceedings of the Ocean Drilling Programme, Scientific Results, 1991, vol. 121, pp. 273–295.
15. Shane, P. A. R., Westgate, J. A., Williams, M. A. J. and Korishetar, R., *Quat. Res.*, 1995, **44**, 200–204.
16. Song, S. R., Chen, C. H., Lee, M. Y., Yang, T. F., Iizuka, Y. and Wie, K. Y., *Mar. Geol.*, 2000, **167**, 303–312.
17. Schulz, H., Von Rad, U. and Erlenkeuser, H., *Nature*, 1998, **393**, 54–57.
18. Buhring, C., Saruthein, M. and Leg 184 Shipboard Scientific Party, *Geology*, 2000, **28**, 275–278.
19. Pattan, J. N., Shane, P., Pearce, N. J. G., Banakar, V. K. and Parthiban, G., *Curr. Sci.*, 2001, **80**, 1322–1326.
20. Ninkovich, D., Shackleton, N. J., Abdel-Monem, A. A., Obradovich, J. D. and Izett, G., *Nature*, 1978, **276**, 574–577.
21. Nambiar, A. R. and Sukumaran, P. V., *J. Geol. Soc. India*, 2002, **59**, 79–88.
22. Chesner, C. A., 1988, Thesis, Michigan Technology University, p. 428.
23. Ledbetter, M. and Sparks, R. S. J., *Geology*, 1979, **7**, 240–244.

24. Woods, A. W. and Wohletz, K., *Nature*, 1991, **350**, 225–227.
25. Zielinski, G. A., Mayewski, P. A., Meeker, L. D., Whitlow, S., Twicker, M. S. and Taylor, K., *Geophys. Res. Lett.*, 1996, **23**, 837–840.
26. Legrand, M. R., Delmas, R. J. and Charlson, R. J., *Nature*, 1988, **334**, 418–420.
27. Lorius, C., Barkov, N. I., Jouzel, J., Korotkevich, Y. S., Kotlyaskov, V. M. and Raymond, D., *EOS*, 1988, **6**, 681–684.

ACKNOWLEDGEMENTS. We are grateful to Dr E. Desa, Director National Institute of Oceanography for permission to publish this work. We thank Mrs Lorraine Hill for assistance. This is NIO contribution No. 3783.

Received 11 February 2002; revised accepted 16 July 2002

Evidence for a female-produced sex pheromone in the banana pseudostem weevil, *Odoiporus longicollis* Olivier

G. Ravi* and M. S. Palaniswami^{†,‡}

*Department of Agricultural Entomology, Agricultural College and Research Institute, Tamil Nadu Agricultural University, Madurai 625 104, India

[†]Division of Crop Protection, Central Tuber Crops Research Institute, Thiruvananthapuram 695 017, India

A female-produced sex pheromone in *Odoiporus longicollis* Olivier was detected in a laboratory bioassay system. Both virgin and mated females produce sex pheromone. There was a significant difference in response of males to females, and it varied towards females of different age groups. The calling behaviour of the females and the courtship behaviour of the males have been documented. This report is an evidence on the presence of sex pheromone in *O. longicollis*.

THE banana pseudostem weevil *Odoiporus longicollis* Olivier (Curculionidae : Coleoptera), has become a serious pest on banana and is distributed mainly in Southeast Asia and New Guinea^{1,2}. In India though it is distributed all over the country, it is a serious pest in the banana-growing belts of Andaman Island³, Uttar Pradesh⁴, Bihar⁵, West Bengal⁶, Assam⁶, Kerala⁷ and Tamil Nadu⁸. The female weevil lays eggs inside the air chamber of the outer sheath of the pseudostem through holes made by its rostrum. Emerging grubs make extensive tunnels in the pseudostem for feeding and pupate in the pseudostem to become adults. Owing to the extensive damage to the pseudostem, it often becomes hollow and weak and bears

[‡]For correspondence. (e-mail: palaniswamims@yahoo.com)